Available online at www.sciencedirect.com
SCIENCE DIRECT
Biochimica et Biophysica Acta 1758 (2006) 636–644
BIOCHIMICA ET BIOPHYSICA ACTA
BBA
http://www.elsevier.com/locate/bba

Preparation and characterization of a stratum corneum substitute for in vitro percutaneous penetration studies

Miranda de Jager [a], Wouter Groenink [a], Joop van der Spek [b], Co Janmaat [c], Gert Gooris [a], Maria Ponec [d], Joke Bouwstra [a,*]

[a] *Leiden/Amsterdam Center for Drug Research, Department of Drug Delivery Technology, Gorlaeus Laboratories, University of Leiden, P.O. Box 9502, 2300 RA Leiden, The Netherlands*
[b] *Fine Mechanical Department, Leiden University, Leiden, The Netherlands*
[c] *Electronic Department, Leiden University, Leiden, The Netherlands*
[d] *Department of Dermatology, Leiden University Medical Center, Leiden, The Netherlands*

Received 17 November 2005; received in revised form 31 March 2006; accepted 3 April 2006
Available online 19 April 2006

Abstract

The intercellular stratum corneum (SC) lipids form the main barrier for diffusion of substances through the skin. A porous substrate covered with synthetic SC lipids would be an attractive model to study percutaneous penetration, hereby replacing native human SC. Prerequisite is that this stratum corneum substitute (SCS) is prepared with a uniform lipid composition and layer thickness. Furthermore, the lipid organization and orientation should resemble that in SC. The objective of this study was to investigate the utility of an airbrush spraying device to prepare a SCS composed of cholesterol, ceramides and free fatty acids on a polycarbonate filter. The results demonstrate that a proper choice of solvent mixture and lipid concentration is crucial to achieve a uniform distribution of the applied lipids over the filter surface. A smooth and tightly packed lipid layer is only obtained when the equilibration conditions are appropriately chosen. The SCS possesses two crystalline lamellar phases with periodicities similar to those present in native SC. The orientation of these lamellae is mainly parallel to the surface of the polycarbonate filter, which resembles the orientation of the intercellular SC lipids. In conclusion, the airbrush technique enables generation of a homogeneous SCS, which ultimately may function as a predictive in vitro percutaneous penetration model.

Keywords: Skin; Permeability; Diffusion; Ceramide; X-ray diffraction

1. Introduction

The nonviable outermost layer of the skin, the stratum corneum (SC), serves as a penetration, dehydration and protection barrier against various environmental hazards. The SC consists of several layers of overlapping corneocytes, embedded in a lipid matrix of ordered lamellae. Despite their overall small percentage, the lipids in the SC represent the main barrier to diffusion of substances. These barrier properties are based on the unique composition and organization of the intercellular lipid lamellae. Ceramides (CER), cholesterol (CHOL) and long-chain free fatty acids (FFA) are the major constituents of the intercellular lamellae [1–4], which are oriented approximately parallel to the surface of the corneocytes [5,6]. These lipids are organized in two coexisting lamellar phases with periodicities of 6 nm (short periodicity phase: SPP) and 13 nm (long periodicity phase: LPP) [7–9]. In particular, the LPP and the crystalline lateral packing are considered to play a crucial role for the skin barrier function.

Recently, there has been an increased interest in drug administration via the skin for both local treatment of the diseased state (dermal delivery) as well as for systemic delivery (transdermal delivery). For this reason, the choice of predictive in vitro test models is important. The use of isolated epidermis or SC sheets from human or animal origin has a number of disadvantages, like high intra- and inter-individual variations and scarcity of the tissue, in particular diseased skin for which numerous topical drug

* Corresponding author. Tel.: +31 71 527 42 08; fax: +31 71 527 45 65.
E-mail address: bouwstra@chem.leidenuniv.nl (J. Bouwstra).

0005-2736/$ - see front matter © 2006 Elsevier B.V. All rights reserved.
doi:10.1016/j.bbamem.2006.04.001

products are designed. In addition, after 2009 there will be an EU-wide ban on the use of animal skin in the testing of cosmetic products. Our ultimate goal is to develop a novel skin barrier model, which can substitute for SC in diffusion studies. The stratum corneum substitute (SCS) consists of a porous substrate covered with specific synthetic SC lipids of uniform composition and layer thickness, mimicking the lipid organization and orientation in SC. Such SCS may function as a standardized and predictive percutaneous penetration model and will therefore circumvent problems related to SC sheets isolated from human or animal skin. Another major advantage of the SCS is that the composition of the synthetic SC lipid mixtures can easily be modified. This allows studying the relation between lipid composition, lipid organization and barrier function in one single model. As a result, important insights may be provided into the defective barrier function and altered SC lipid composition and organization underlying various skin diseases [10–13]. Ultimately, a SCS may be prepared that mimics not only healthy, but also diseased and dry skin, for which there is currently no alternative screening system available.

To mimic the SC barrier function, the SCS should meet the following requirements: (i) the lipids should spread homogeneously over the entire substrate surface. This is important for the formation of the characteristic LPP and the crystalline lateral packing [14–16]. (ii) The lipid layer should have a uniform thickness. Furthermore, cracks or holes should be absent, as these defects will disrupt the barrier properties. (iii) The orientation of the lamellae should be parallel to the substrate surface, which mimics the situation in native SC. (iv) The lipids should be organized in the LPP and SPP with an orthorhombic lateral packing, similarly as observed in SC.

In previous studies, we have already demonstrated that the unique SC lipid organization, including the 13 nm lamellar phase, can be reproduced in vitro with mixtures based on cholesterol, free fatty acids, and synthetic ceramides (synthCER), provided that the lipid composition and equilibration temperature are appropriately chosen [17–19]. The objective of the present study was to explore the possibility of preparing a SCS with an airbrush. This was performed by spraying equimolar mixtures of cholesterol, synthetic ceramides and free fatty acids onto a polycarbonate filter. The SCS was subsequently characterized in terms of distribution of the lipid classes over the substrate surface, homogeneity of the lipid layer, and orientation and organization of the lipid lamellae. For these purposes, high performance thin layer chromatography, cryo-scanning electron microscopy, low-angle and wide-angle X-ray diffraction were used.

2. Materials and methods

2.1. Materials

CER(EOS)C30-linoleate, CER(NS)C24, CER(NP)C24, CER(NP)C16, CER(AS)C24 and CER(AP)C24 were generously provided by Cosmoferm B.V. (Delft, The Netherlands). Palmitic acid, stearic acid, arachidic acid, behenic acid, tricosanoic acid, lignoceric acid, cerotic acid and cholesterol were purchased from Sigma-Aldrich Chemie GmbH (Schnelldorf, Germany). Nuclepore polycarbonate filter disks (pore size 50 nm) were purchased from Whatman (Kent, UK). All organic solvents used were of analytical grade and manufactured by Labscan Ltd. (Dublin, Ireland). All other chemicals were of analytical grade and the water used was of Millipore quality.

2.2. Preparation of the SCS

For the preparation of the synthCER mixture, CER(EOS), CER(NS), CER(NP)C24, CER(AS), CER(NP)C16 and CER(AP) were mixed in a 15:51:16:4:9:5 molar ratio, which closely resembles the composition of the ceramides in pig SC [14,20]. For the preparation of the free fatty acids mixtures, the following fatty acid mixture was used: C16:0, C18:0, C20:0, C22:0, C23:0, C24:0 and C26:0 at molar ratios of 1.3, 3.3, 6.7, 41.7, 5.4, 36.8 and 4.7, respectively. This is similar to the free fatty acids composition in SC [21]. Appropriate amounts of individual lipids dissolved in chloroform:methanol (2:1) were combined to yield lipid mixtures at the desired equimolar CHOL:synthCER:FFA composition. After evaporation of the organic solvent under a stream of nitrogen, the lipid mixtures were re-dissolved in either hexane:isopropanol (3:2), methanol:ethylacetate (2:1) or hexane:ethanol (2:1) at a total lipid concentration of 2 or 4.5 mg/ml.

An evolution solo airbrush (Airbrush Service Almere, The Netherlands) connected to gaseous nitrogen was used to spray the lipid mixtures onto a polycarbonate filter disk with a pore size of 50 nm. Briefly, the porous substrate was mounted in a holder and fixed under the airbrush, which was constructed vertically with the nozzle facing downwards. The reservoir of the airbrush was subsequently filled with the lipid solution. The device enables us to control: (i) the spraying period. During the spraying period, the trigger is opened pneumatically for a certain adjustable time period, during which a small fraction of the lipid solution passes the nozzle. Due to this nitrogen pressure, the lipid solution is sprayed in very small droplets onto the porous substrate. The distance over which the trigger is opened can be adjusted accurately with a micrometer screw. (ii) The drying period, which follows the spraying period. During the drying stage, the trigger is closed, the organic solvent evaporates by the nitrogen flow and the lipids attach to the substrate. To ensure proper spreading of the lipids, the nitrogen pressure during the spraying and the drying stage can be regulated independently. This has been achieved by making use of an air valve, which assures a high pressure during spraying and a low pressure during drying. (iii) Multiple application. The number of spraying and drying cycles is adjustable to obtain the required layer thickness. Prior to the spraying stage, the nitrogen pressure is increased to levels required for appropriate spraying. The equipment settings that were used are listed in Table 1, whereas a schematic representation of the application set-up is illustrated in Fig. 1. After preparation, the lipid-loaded filters were equilibrated at 70 °C, for a period of 10 min. If required, hydration of the lipid membranes under buffer was performed by applying an excess of an acetate buffer of pH 5.0 after the equilibration step.

2.3. Lipid distribution

One-dimensional high performance thin layer chromatography was used to establish the distribution of the various lipid classes over the filter surface. Briefly, the lipid-loaded filters were cut into two circular parts: the centre (diameter 4 mm; area 12.6 mm^2) and the periphery (diameter 9 mm; area 51.0 mm^2). The lipids were extracted in 0.5 ml chloroform:methanol (2:1) by extensive vortexing and were subsequently re-dissolved in ratios according to the surface area. Aliquots were applied on a silica plate (Merck, Darmstadt, Germany) under a flow of nitrogen using a Camag Linomat IV (CAMAG, Muttenz, Switzerland). After eluting with different organic solvent mixtures [22], the silica plate was sprayed with copper sulfate. After charring, the intensities of the lipid bands were determined using a photodensiometer with automatic peak integration (Biorad GS 710, Hercules, USA).

Table 1
Equipment settings used for spraying of the SCS

Parameter	Setting
Pressure during spraying (above atmospheric pressure)	1.16 bar
Time trigger open	1 s
Distance over which the trigger is opened	5.5 mm
Pressure during drying (above atmospheric pressure)	160 mbar
Time trigger closed	15 s
Distance between the nozzle and the filter	4.5 cm

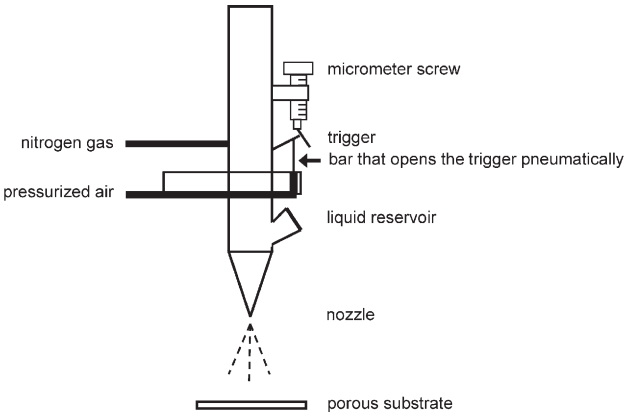

Fig. 1. A schematic presentation of the airbrush. During the spraying period, the trigger of the airbrush is opened pneumatically by a bar (indicated with an arrow). After the spraying period, the air pressure drops, the bar goes down, the trigger is closed, and the liquid supply immediately stops.

2.4. Homogeneity of lipid layer

Cryo-scanning electron microscopy was used to establish the compactness of the lipid layer of lipid membranes that were (i) equilibrated and hydrated, (ii) not equilibrated and not hydrated, (iii) equilibrated but not hydrated or (iv) equilibrated and cooled to room temperature prior to hydration. Prior to processing the specimens for cryo-scanning electron microscopy, hydrated lipid membranes were all exposed to the buffer solution for at least 20 h. Subsequently, the lipid-loaded filters were cut into sheets of 1.5×2 mm^2, folded and fixed in a small copper "shoe-nail" using Tissue-Tek O.C.T. Compound (Miles Inc. Elkhart, IN, USA). The samples were then quickly frozen by plunge-freezing (Reichert Jung-KF80, Vienna, Austria) into liquid propane at −180 °C. The frozen specimens were kept in liquid nitrogen until mounting into a sample holder. The cryofixed samples were planed in a cryo ultramicrotome (Leica Ultracut UCT/Leica EM FCS, Wetzlar, Germany), using a specimen temperature of −90 °C and a knife temperature of −100 °C [23]. Subsequently, the samples were vacuum dried for 3 min at −90 °C at 0.1 Pa to obtain contrast and sputtered with a layer of platinum (CT 1500 HF, Oxford Instruments, UK). After transferring the specimens into the field emission scanning electron microscope (Jeol 6400F, Tokyo, Japan), the samples were visualized at −190 °C. At least 5 electron micrographs were taken from each lipid-loaded filter and at least 2 lipid-loaded filters were prepared per condition.

2.5. Correlation between the layer thickness and the quantity of lipid material

To establish the correlation between the quantity of lipid material and the resulting layer thickness, filters were covered with approximately 0.5, 0.8, 1.2 and 1.5 mg/cm^2 of lipid material and were subsequently equilibrated. Three lipid-loaded filters were prepared and examined per experimental condition. Briefly, circular lipid-loaded filter pieces (diameter 6 mm; area 12.6 mm^2) were cut into two equally sized parts. One part was dissolved in 100 μl chloroform/methanol (2:1) and the lipids were extracted by extensive vortexing. After evaporation of the organic solvent, the amount of lipids was determined by weighing. The other part was used for cryo-scanning electron microscopy to establish the thickness and compactness of the lipid layer. At least 4 microscopic images were taken from each lipid-loaded filter. At equal distances of 20 μm along the cutting plane, the thickness of the cross-section of each lipid layer was determined by establishing the pixel position of the top and bottom of the lipid layer in proportion to that of the magnification bar that is present in each micrograph.

2.6. Orientation and organization of lipid lamellae

Low-angle X-ray diffraction was used to acquire information about the lamellar organization (i.e., the repeat distance of a lamellar phase) and the orientation of the lamellae. The scattering intensity I (in arbitrary units) was measured as a function of the scattering vector q (in reciprocal nm). The latter is defined as $q=(4\pi sin\theta)/\lambda$, in which θ is the scattering angle and λ is the wavelength. From the positions of a series of equidistant peaks (q_n), the periodicity, or d-spacing, of a lamellar phase was calculated using the equation $q_n=2n\pi/d$, n being the order number of the diffraction peak. A preferred orientation of the lamellae parallel to the substrate surface is indicated by small arcs on the detection plane with a maximum intensity at the meridian, whereas disoriented lamellae result in full rings of equal intensity.

All measurements were performed at the European Synchrotron Radiation Facility (ESRF, Grenoble) using station BM26B [24]. The X-ray wavelength and the sample-to-detector distance were 0.124 nm and 1.7 m, respectively. Diffraction data were collected on a two-dimensional multiwire gas-filled area detector with 512×512 pixels of 0.25 mm spatial resolution. The spatial calibration of this detector was performed using silver behenate (d=5.838 nm). A filter with lipid layers was mounted parallel to the primary beam in a temperature-controlled sample holder with mica windows. Static diffraction patterns were obtained at room temperature for a period of 5 min. The temperature-induced phase changes were investigated by collecting diffraction patterns, while the temperature of the sample was raised to 75 °C at a rate of 2°/min. Each successive diffraction curve was collected for a period of 1 min.

Wide-angle X-ray diffraction provides information about the lateral packing of the lipids within the lamellae. Data were collected on a microstrip gas chamber detector with an opening angle of 60° [25]. The sample-to-detector distance was 36 cm and the X-ray wavelength was 1.24 Å. The spatial calibration of the detector was performed with a mixture of Silicium (d=0.3136 nm) and cholesterol (d=3.36 nm).

3. Results

3.1. Lipid distribution

Polycarbonate filters are not resistant towards chloroform. Therefore, three alternative organic solvent mixtures were selected

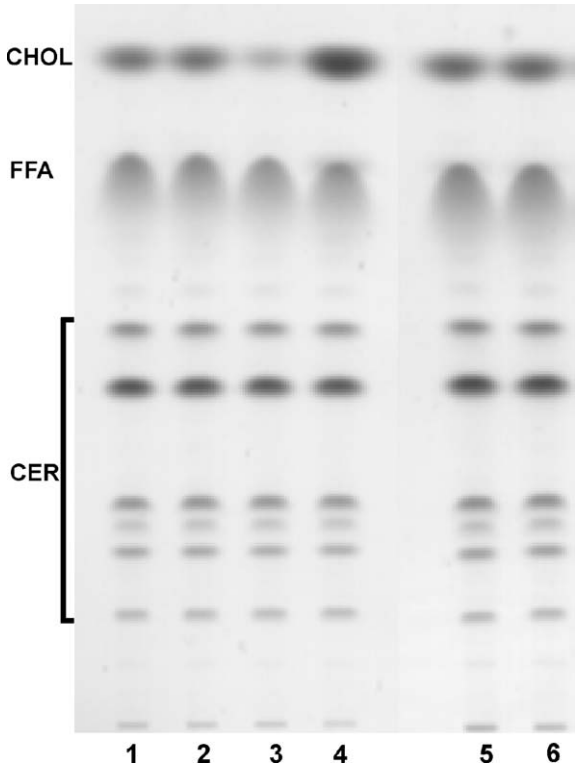

Fig. 2. Lipid distribution from three solvent mixtures at a total lipid concentration of 4.5 mg/ml. 1=centre M/EA; 2=periphery M/EA; 3=centre H/IPA; 4=periphery H/IPA; 5=centre H/Et; 6=periphery H/Et.

to dissolve the lipids, namely methanol:ethylacetate (M:EA), hexane:isopropanol (H:IPA) and hexane:ethanol (H:Et). Filters were covered with approximately 0.25 mg/cm^2 and 0.5 mg/cm^2 of lipid material. Whereas the total amount of lipids applied on the filter does not have an effect on the distribution (data not shown), the solvent mixture and total lipid concentration markedly affect the lipid distribution, in particular that of cholesterol. Fig. 2 shows the lipid distribution of the lipid subclasses between the filter centre and periphery, making use of the three organic solvent mixtures at a total lipid concentration of 4.5 mg/ml. From the intensities of the bands, it is obvious that an even distribution of cholesterol is only obtained when the lipids are dissolved in H:Et or M:EA. When H:IPA is used as a solvent, the amount of cholesterol present at the filter periphery is nearly 6- to 8-fold higher than the amount present in the central part. With 2 mg/ml solutions an inhomogeneous distribution of the lipid classes is observed with all three solvent mixtures (data not shown), similarly as the distribution obtained with H:IPA at 4.5 mg/ml solution.

Although the distribution of the lipids from H:Et and M:EA solutions is comparable, a considerable improvement of the spraying process is obtained when the lipids are dissolved in H:Et. Moreover, the lipid loss during application is slightly lower, which can most likely be ascribed to the lower solubility of the lipids in M:EA as compared to H:Et. For this reason, all further experiments were performed with lipid solutions in H:Et at a total lipid concentration of 4.5 mg/ml.

3.2. Compactness of the lipid layer

Fig. 3A shows an electron micrograph of a cross-section of a lipid membrane and the underlying polycarbonate filter, equilibrated at 70 °C and subsequently hydrated with an acetate buffer. It can be clearly observed that this procedure, which is routinely used to obtain proper lipid organization in synthetic lipid mixtures for X-ray diffraction measurements, results in the formation of large holes in the lipid layer. To elucidate whether the holes are caused by the elevated temperature during equilibration or by the successive addition of the acetate buffer, filters were covered with approximately 0.5 mg/cm^2 of lipid material and the lipid membranes were either (i) not equilibrated and not hydrated (Fig. 3B), (ii) equilibrated but not hydrated (Fig. 3C), or (iii) equilibrated and cooled to room temperature prior to hydration (Fig. 3D).

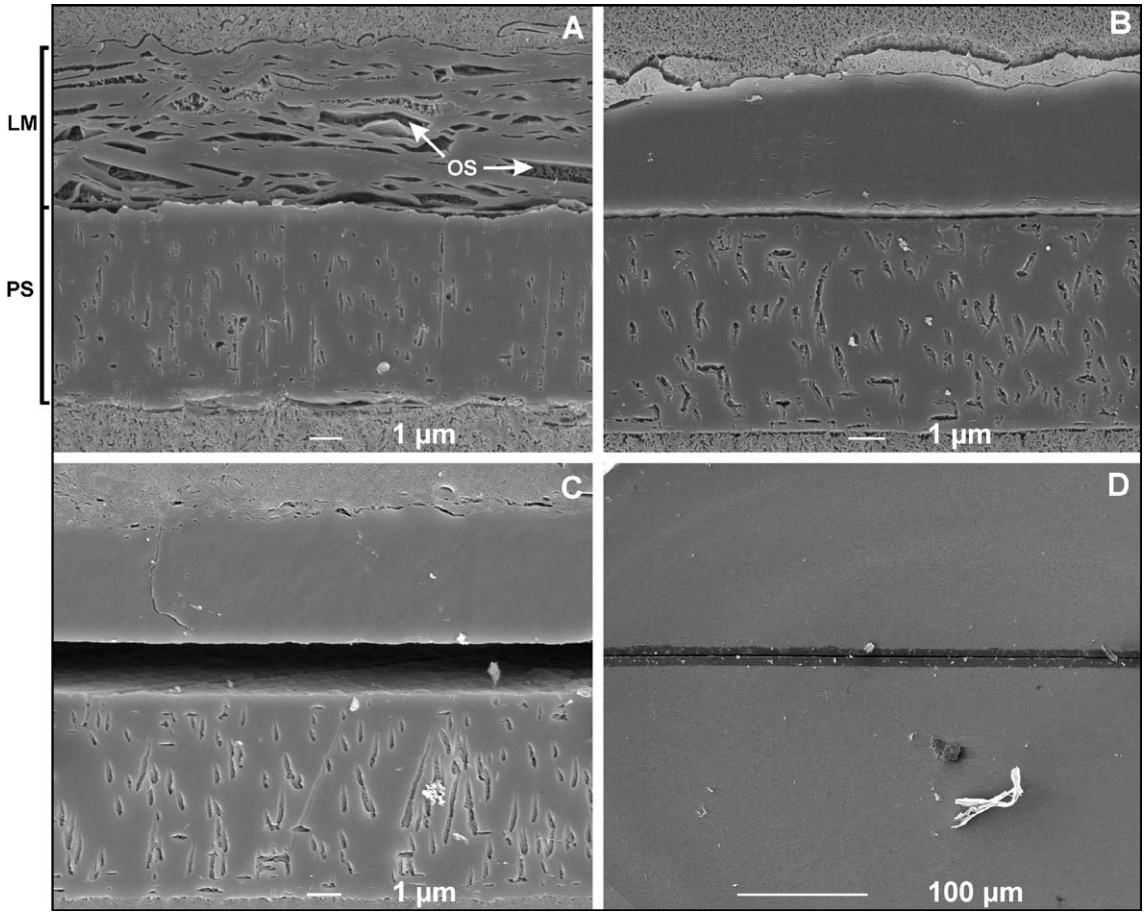

Fig. 3. Cryo-scanning electron microscopy photographs of cross-sections of lipid membranes (LM) and underlying porous substrates (PS). (A) Lipid membrane that was equilibrated and hydrated (large open structures (OS) can be observed in the lipid layer); (B) Lipid membrane that was not equilibrated and not hydrated; (C) Lipid membrane that was equilibrated, but not hydrated. The detachment of the lipid layer from the polycarbonate filter is most likely an artefact, which arose during the preparation of this specimen for electron microscopy; (D) Lipid membrane that was equilibrated and cooled to room temperature prior to hydration (lower magnification).

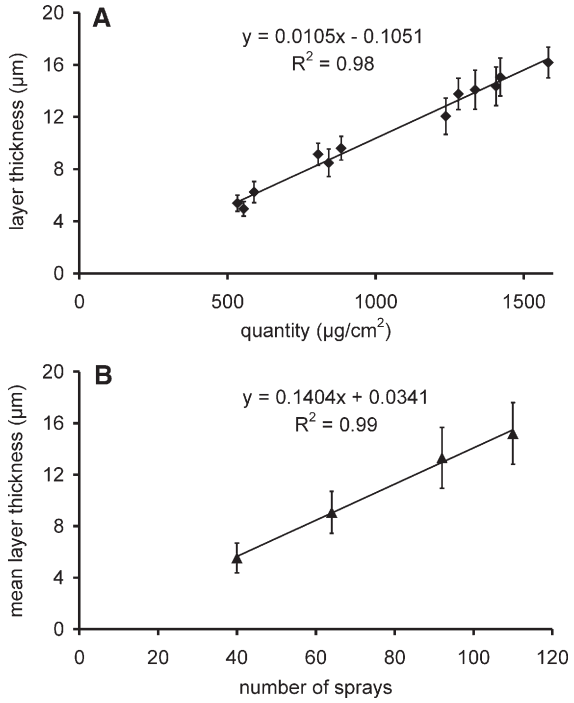

Fig. 4. The correlation between the layer thickness and quantity of lipid material (A) and the correlation between the average layer thickness and the number of sprays (B).

The results indicate that when the buffer is applied directly after the equilibration step, it is able to penetrate the lipid membrane, where it phase separates to form water-rich domains. Because the samples were vacuum dried for a short period prior to visualization, the water-rich domains are consequently visualized as holes in the lipid layer.

No significant differences can be observed between the lipid membranes presented in Fig. 3B–D. All preparation methods result in the formation of a tightly packed lipid layer in the absence of large open structures. In addition, no lipid material is present inside the pores or at the bottom side of the filter. From Fig. 3D, in which a lower magnification of the lipid membrane and the underlying filter is presented, it can further be deduced that also over a larger surface area the lipid membranes have a uniform layer thickness.

3.3. Correlation between layer thickness and quantity of lipid material

Fig. 4A demonstrates that an almost linear relationship exists between the layer thickness and the quantity of lipid material of individual lipid membranes (correlation coefficient = 0.98). The layer thickness of each individual lipid membrane as well as the quantity of lipid material applied per filter is highly reproducible and only slightly fluctuates with steady relative standard deviations of 10% and 5%, respectively.

From the slope of the line in Fig. 4B, in which the average layer thickness is plotted against the number of sprays required to obtain that particular layer thickness, it can be observed that approximately 0.14 µm of lipid material is applied onto the filter per spray.

3.4. Orientation and organization

Fig. 5A shows a typical two-dimensional X-ray diffraction pattern of a non-hydrated lipid membrane. The arcs on the detection plane, having a maximum intensity at the meridian, indicate a preferred orientation of the lamellae parallel to the polycarbonate filter. Sector integration (angle 60°) resulted in Fig. 5B, in which the intensity of the arcs is plotted versus the scattering vector q. The LPP with a repeat distance of 12.2 nm is indicated by the presence of five reflections (q = 0.52, 1.03, 1.54, 2.06 and 3.08 nm^{-1}). The reflections at q = 1.18, 2.36 and

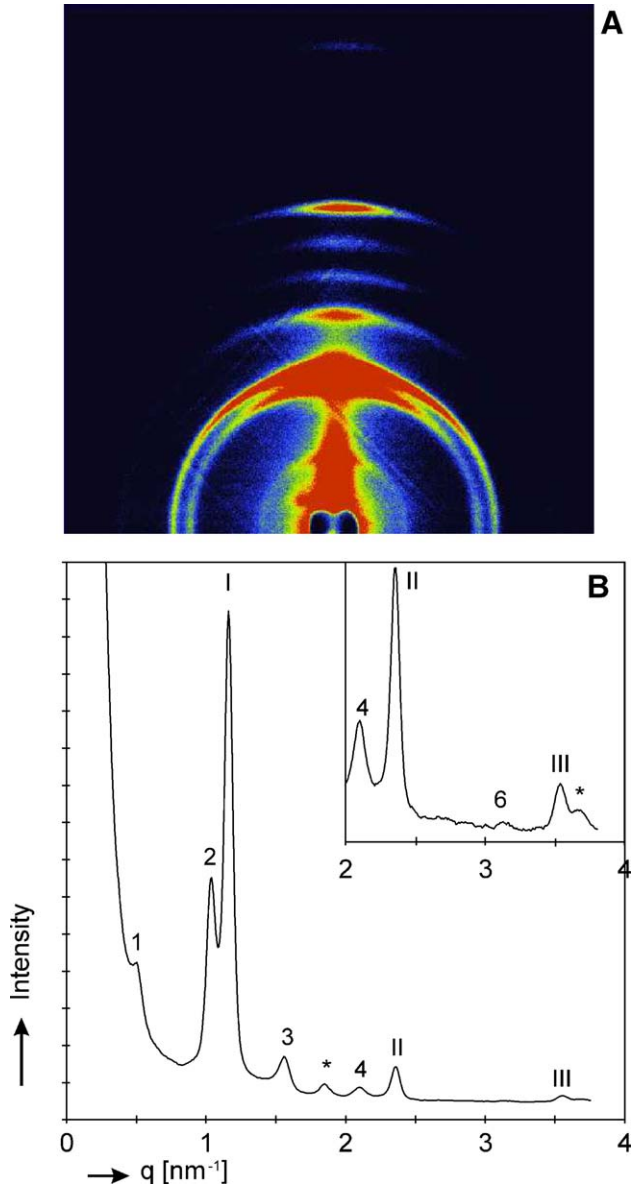

Fig. 5. The orientation (A) and lamellar organization (A and B) of a non-hydrated lipid membrane. The inset shows a magnification of the reflections in the q-range between 2 and 4 nm^{-1}. The Arabic and Roman numbers indicate the diffraction orders of the LPP and SPP, respectively. The asterisk (*) indicates the reflections of crystalline cholesterol located at 1.87 and 3.74 nm^{-1}. The various orders of the LPP are located at q = 0.52 nm^{-1} (1), 1.03 nm^{-1} (2), 1.54 nm^{-1} (3), 2.06 nm^{-1} (4), and 3.08 nm^{-1} (6). The various orders of the SPP are located at q = 1.18 nm^{-1} (I) and 2.36 nm^{-1} (II), and 3.53 nm^{-1} (III).

3.53 nm^{-1} correspond to the first, second and third order diffraction peaks of a lamellar phase with a periodicity of 5.4 nm (SPP). The presence of crystalline cholesterol in separate domains can be deduced from the peaks at 1.86 and 3.72 nm^{-1}. No significant differences in the orientation or lamellar organization could be observed between hydrated and non-hydrated lipid membranes.

The lamellar and lateral lipid phase behavior of the non-hydrated and hydrated lipid membranes was also studied as a function of temperature (Fig. 6A–D). Each curve represents the mean of the lipid phases present during a temperature shift of 2 °C. The diffraction patterns illustrated in Fig. 6A (non-hydrated lipid membranes) and Fig. 6B (hydrated lipid membranes) reveal a number of reflections that can be ascribed to the presence of the LPP (12.2 nm) and SPP (5.4 nm), similarly as described in Fig. 5. In addition, crystalline cholesterol is present in separate domains. No significant changes are observed in the intensities or positions of the reflections of the phases between 25 and 51 °C. However, the reflections of the LPP disappear at around 65 °C. Despite these similarities, two differences in the lamellar organization are observed between non-hydrated and hydrated lipid membranes. Firstly, in hydrated lipid membranes the two reflections attributed to crystalline cholesterol disappear at around 57 °C, whereas in non-hydrated lipid membranes, it is reproducibly observed that the cholesterol reflections disappear only at approximately 73 °C. Secondly, in hydrated lipid

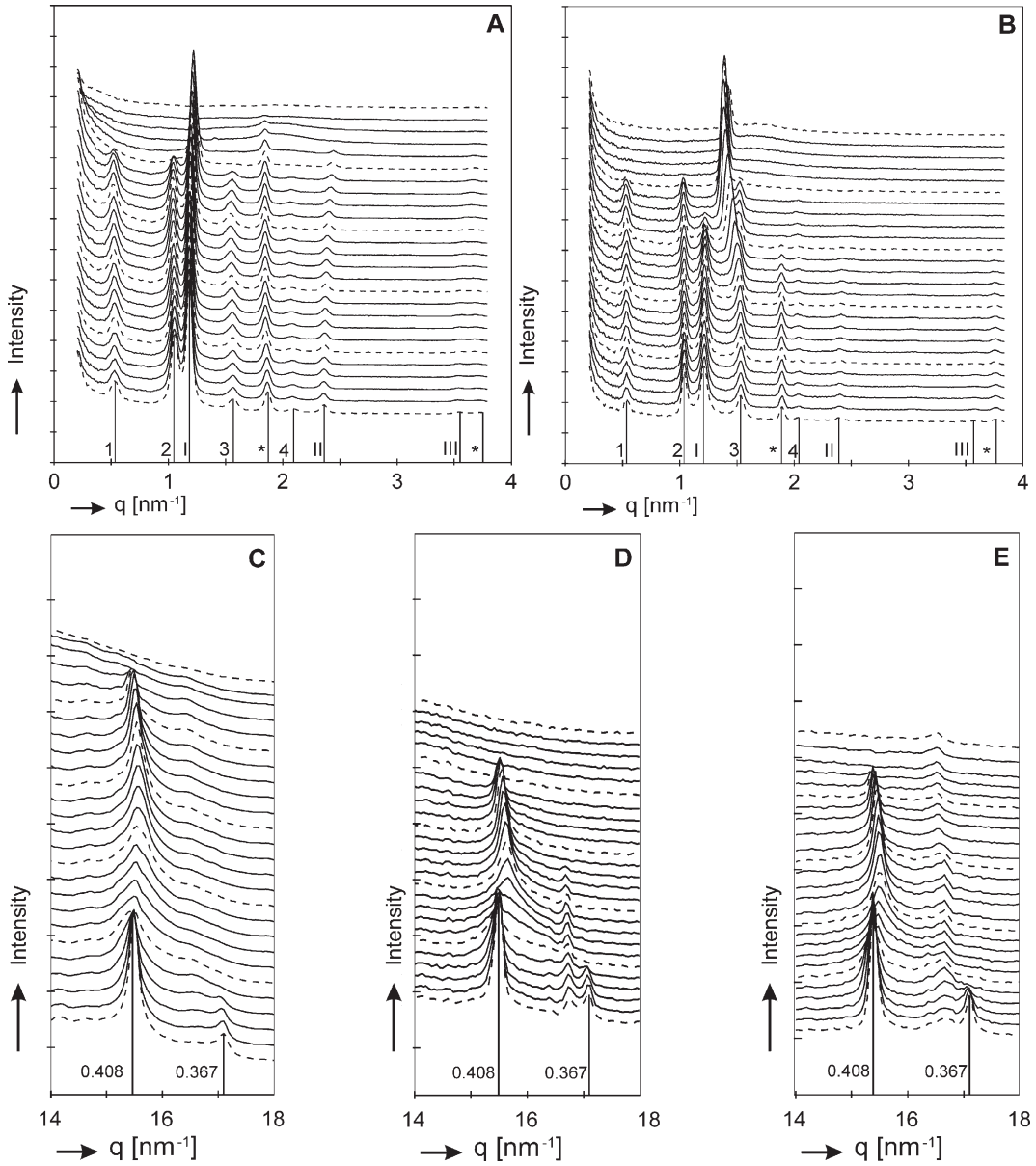

Fig. 6. Temperature-induced changes in (A) the lamellar lipid organization of a non-hydrated lipid membrane, (B) the lamellar lipid organization of a hydrated lipid membrane, (C) the lateral lipid organization of a non-hydrated lipid membrane, (D) the lateral lipid organization of a hydrated lipid membrane, and (E) the lateral lipid organization of isolated human SC. The Arabic and Roman numbers indicate the diffraction orders of the LPP and SPP, respectively. The asterisk (*) indicates the reflections of crystalline cholesterol. The dashed lines represent the diffraction curves at 25, 35, 45, 55, 65, and 75 °C.

membranes the reflections of the SPP disappear at around 51 °C. In the same temperature range, a new phase is formed, of which only one reflection can be detected that gradually shifts to $q=1.37\ nm^{-1}$ (repeat distance 4.6 nm). In non-hydrated lipid membranes, however, the reflections of the SPP do not disappear at elevated temperatures and in addition no additional phase with a repeat distance of 4.6 nm is formed. Previous studies performed with mixtures based on isolated ceramides have shown that the formation of the additional phase at elevated temperatures is strongly related to the amount of cholesterol that is available for the formation of this phase [26]. For hydrated lipid membranes, it can be observed that the formation of the additional 4.6 nm phase is in the same temperature region in which the reflections of phase-separated cholesterol disappear. The cholesterol reflections in non-hydrated lipid mixtures disappear at a much higher temperature than in hydrated lipid membranes. Hence the amount of available cholesterol is most likely insufficient for the formation of the 4.6 nm phase. In isolated human SC the formation of this additional phase at elevated temperatures is also hardly ever observed [26], which once again demonstrates the high similarity in lipid phase behavior between SC and the SCS.

A hexagonal lateral packing is characterized by a strong 0.41 nm reflection in the wide-angle X-ray diffraction pattern, whereas the diffraction pattern of an orthorhombic packing is characterized by two strong 0.41 and 0.37 nm reflections. The diffraction patterns of non-hydrated and hydrated lipid membranes monitored as a function of temperature are plotted in Fig. 6C and D, respectively. Fig. 6E, in which the diffraction pattern of isolated human SC as a function of temperature is illustrated, serves as a control. Both non-hydrated and hydrated lipid membranes show similar behavior as isolated human SC. The 0.408 and 0.367 nm peaks indicate an orthorhombic lateral packing. At around 33 °C, the 0.367 nm reflection disappears, indicating an orthorhombic to hexagonal phase transition. The 0.408 nm reflection first decreases in intensity. However, a further rise in temperature increases the intensity of the 0.408 nm reflection slightly, indicating a metastable to stable phase change. This phenomenon is also observed in the diffraction patterns of SC (see Fig. 6E). A disappearance of this peak is observed at 65 °C, which is in the same temperature range at which the LPP disappears in the low-angle X-ray diffraction patterns. The reflection, which is located at approximately $q=16.6\ nm^{-1}$ in Fig. 6D and disappears at around 57 °C can be ascribed to crystalline cholesterol [14]. This is confirmed by the results presented in Fig. 6B, in which two other reflections attributed to crystalline cholesterol disappear in the same temperature range.

4. Discussion

The objective of the present study was to evaluate the possibility of preparing a SCS, which closely resembles the composition, organization and orientation of the intercellular lipids in SC. As the resulting SCS may ultimately function as a percutaneous penetration model, it is further important that the lipids of the SCS are tightly packed and have a uniform layer thickness. These various aspects are discussed below.

4.1. Uniform lipid distribution

The results of the present study show that both the organic solvent mixture and the total lipid concentration are important determinants for successful preparation of a SCS of uniform lipid composition. It should be stressed, however, that the equipment settings used for the preparation of the SCS are at least as important as the two aforementioned factors. The most critical parameters in this respect are the distance between the nozzle of the airbrush and the filter, the nitrogen pressure during the spraying and drying stage, and the quantity of lipid solution that passes the nozzle per spray. One can state that the evaporation rate during the drying stage should balance the quantity of lipid solution that reaches the polycarbonate filter during the preceding spraying stage.

When the process conditions were not optimally chosen, the evaporation process of the organic solvent occurred from the inside to the periphery and sometimes the lipid solution itself was even blown to the filter periphery. The latter phenomenon was specifically observed when the nitrogen pressure during the drying stage was set too high or when the evaporation velocity was too slow for the supply of lipid solution (e.g., by preparing lipid solutions at a total lipid concentration of 2 mg/ml). In either case, cholesterol was mainly present at the periphery of the lipid membrane, whereas the central part hardly contained any cholesterol (see also Fig. 2). The solubility of cholesterol in the organic solvent mixtures is higher than that of the synthetic ceramides and free fatty acids. During the evaporation process of the organic solvent, the concentration of the lipids increases and the lipids crystallize according to their solubility. Cholesterol therefore remains in solution up to the edges of the lipid membrane. Interestingly, this could sometimes even be visually observed by a small band of crystals. On the other hand, when the supply of lipid solution was set too low, most of the organic solvent already evaporated before the lipid solution reached the filter. Due to substantial lipid loss, only a small area of the filter could be covered with lipid material.

4.2. Compactness of the lipid layer

The airbrush spraying technique results in the formation of smooth and tightly packed lipid membranes, provided that the hydration step, which immediately follows the equilibration step, is omitted. As demonstrated by the X-ray diffraction data, omission of the hydration step does not affect the lamellar or lateral lipid organization. It has to be kept in mind, however, that during a diffusion experiment, non-hydrated lipid membranes will be exposed to a donor and an acceptor solution for several hours. In order to guarantee proper barrier function, it is necessary that the SCS remains intact under those conditions. Preliminary studies indicate that the SCS remains intact for a period of at least 20 h during a diffusion experiment.

The results of the present study demonstrate that lipid membranes that are first cooled to room temperature prior to hydration do not possess large holes, indicating that no water pools are formed in the lipid membranes at room temperature. This finding is crucial, as these defects would disrupt the barrier properties of the SCS.

For preparation of a homogeneous SCS it is further important that the lipid layer is only present on top of the filter and not inside the pores of the filter. Filled or partially filled pores are easily recognizable by the fact that pores are not at all visible over the entire length of the filter, up to a certain depth. However, electron microscopy studies on lipid membranes prepared at the optimal equipment settings evidently demonstrate that the lipids are able to span the pores of the supporting membrane, as no lipid material is present inside the pores or at the bottom side of the filter. The results further demonstrate that a uniform layer thickness and penetration pathway for substances can be obtained and established. This will considerably facilitate the interpretation of future diffusion results.

4.3. Orientation of the lipid lamellae

The orientation of the lipid lamellae in the lipid membranes is parallel to the surface of the hydrophilic polycarbonate filter. From the width of the arcs, however, it cannot be excluded that some disorientation exists. Previous X-ray diffraction measurements on isolated human SC reveal that the orientation of the intercellular lamellae is also not exactly parallel to the skin surface (Bouwstra J.A., Gooris, G.S., unpublished data). The width of the arcs of the SCS approximates that of SC rather closely, indicating that the synthetic lipids in the SCS resemble the orientation of the intercellular lipids in the SC. In vivo, the monolayer of covalently bound lipids surrounding each corneocyte is often suggested to serve as a template in the assembly of the multilamellar structures parallel to the corneocyte surface [27]. The SCS is solely composed of synthetic SC lipids and does not contain any corneocytes. Nonetheless, the orientation of the lipid lamellae is found to be mainly parallel to the filter surface, which suggests that one lipid layer forms a template for the next layer. Inspection of literature reveals that the airbrush has also been used successfully for the preparation of aligned samples of phospholipids [28,29].

4.4. Lipid composition and organization

Although the method of lipid analysis used in the present study did not allow the investigation of the lipid distribution as a function of depth, previous studies have shown that the lipid organization is not extremely sensitive towards changes in the total CHOL:synthCER:FFA molar ratio [9,30]. For this reason, small variations in the lipid composition will presumably not affect the lipid organization to a high extent.

The results of the present study reveal that the LPP (12.2 nm) and SPP (5.4 nm) are both present in non-hydrated and hydrated lipid membranes. Moreover, an orthorhombic lateral packing of the lipids is observed in both non-hydrated and hydrated lipid membranes. This indicates that only the equilibration temperature and no hydration is important for proper lamellar and lateral lipid organization. This finding is of crucial importance, as only in non-hydrated lipid membranes the lipid layer is tightly packed. The periodicities of the lamellar phases in hydrated and non-hydrated lipid membranes are exactly the same. This is in good agreement with previous X-ray diffraction measurements on hydrated SC [7,8] and lipid mixtures prepared with isolated ceramides [31] in which an increased hydration level did not result in significant lamellar swelling. However, McIntosh et al. found that mixtures of isolated ceramides prepared in the absence of water are more sensitive to phase separation of cholesterol than hydrated lipid mixtures of the same composition [31]. This may explain the small differences in the lamellar lipid organization of non-hydrated and hydrated lipid membranes at elevated temperatures. Studies performed in our group revealed that only in the presence of a buffer the phase behavior of mixtures prepared with isolated ceramides is similar to that in SC (de Jager, M.W., Gooris, G.S., Ponec, M. and Bouwstra J.A., unpublished data).

In conclusion, the present study has shown that the airbrush is an elegant apparatus to homogeneously spray reconstituted synthetic SC lipids onto a porous polycarbonate filter, provided that the experimental conditions used for spraying as well as for equilibration are appropriately chosen. As the SCS prepared in the present study has a uniform lipid layer thickness and further closely resemble the composition, organization and orientation of the intercellular lipids in SC, they may have a great potential to ultimately serve as a novel skin barrier diffusion model. The barrier properties of the SCS will therefore be investigated in a future study.

Acknowledgements

This work was supported by a grant from the Technology Foundation STW (LGN4654). The Netherlands Organization for Scientific Research (NWO) is acknowledged for the provision of the beamtime. The authors wish to express their gratitude to I.P. Dolbnya and W. Bras for their valuable contribution at the ESRF. We would like to thank the company Cosmoferm B.V. for the provision of the synthetic ceramides and Raphaël Zwier (Fine Mechanical Department, Leiden University) for manufacturing the filter holders.

References

[1] P.W. Wertz, M.C. Miethke, S.A. Long, J.S. Strauss, D.T. Downing, The composition of the ceramides from human stratum corneum and from comedones, J. Invest. Dermatol. 84 (1985) 410–412.
[2] K.J. Robson, M.E. Stewart, S. Michelsen, N.D. Lazo, D.T. Downing, 6-Hydroxy-4-sphingenine in human epidermal ceramides, J. Lipid Res. 35 (1994) 2060–2068.
[3] M.E. Stewart, D.T. Downing, A new 6-hydroxy-4-sphingenine-containing ceramide in human skin, J. Lipid Res. 4 (1999) 1434–1439.
[4] M. Ponec, A. Weerheim, P. Lankhorst, P. Wertz ,New acylceramide in native and reconstructed epidermis, J. Invest. Dermatol. 120 (2003) 581–588.
[5] K.C. Madison, D.C. Schwartzendruber, P.W. Wertz, D.T. Downing, Presence of intact intercellular lipid lamellae in the upper layers of the stratum corneum, J. Invest. Dermatol. 88 (1987) 714–718.
[6] D.C. Swartzendruber, P.W. Wertz, D.J. Kitko, K.C. Madison, D.T. Downing, Molecular models of intercellular lipid lamellae in mammalian stratum corneum, J. Invest. Dermatol. 92 (1989) 251–257.
[7] J.A. Bouwstra, G.S. Gooris, J.A. van der Spek, W. Bras, The structure of human stratum corneum as determined by small angle X-ray scattering, J. Invest. Dermatol. 96 (1991) 1006–1014.
[8] J.A. Bouwstra, G.S. Gooris, J.A. van der Spek, W. Bras, Structural investigations of human stratum corneum by small angle X-ray scattering, J. Invest. Dermatol. 97 (1991) 1005–1012.
[9] J.A. Bouwstra, G.S. Gooris, W. Bras, D.T. Downing, Lipid organization in pig stratum corneum, J. Lipid Res. 36 (1995) 685–695.

[10] A. Di Nardo, P. Wertz, A. Giannetti, S. Seidenari, Ceramide and cholesterol composition in the skin in patients with atopic dermatitis, Acta Derm. Venereol. (Stockh.) 78 (1998) 27–30.
[11] S. Motta, M. Monti, S. Sesana, R. Caputo, S. Carelli, R. Ghidoni, Ceramide composition of the psoriatic scale, Biochim. Biophys. Acta 8 (1993) 147–151.
[12] Y. Yamamoto, S. Serizaka, M. Ito, Y. Sato, Stratum corneum lipid abnormalities in atopic dermatitis, Arch. Dermatol. Res. 283 (1991) 219–223.
[13] A.P.M. Lavrijsen, J.A. Bouwstra, G.S. Gooris, H.E. Boddé, M. Ponec, Reduced skin barrier function parallels abnormal stratum corneum lipid organization in patients with lamellar ichthyosis, J. Invest. Dermatol. 105 (1995) 619–624.
[14] J.A. Bouwstra, G.S. Gooris, K. Cheng, A. Weerheim, W. Bras, M. Ponec, Phase behavior of isolated skin lipids, J. Lipid Res. 37 (1996) 999–1011.
[15] J.A. Bouwstra, G.S. Gooris, F.E.R. Dubbelaar, M. Ponec, Phase behavior of lipid mixtures based on human ceramides: coexistence of crystalline and liquid phases, J. Lipid Res. 42 (2001) 1759–1770.
[16] J.A. Bouwstra, G.S. Gooris, F.E.R. Dubbelaar, M. Ponec, Phase behavior of stratum corneum lipid mixtures based on human ceramides: the role of natural and synthetic ceramide 1, J. Invest. Dermatol. 118 (2002) 606–617.
[17] M.W. de Jager, G.S. Gooris, I.P. Dolbnya, W. Bras, M. Ponec, J.A. Bouwstra, Novel lipid mixtures based on synthetic ceramides reproduce the unique stratum corneum lipid organization, J. Lipid Res. 45 (2004) 923–932.
[18] M. de Jager, G. Gooris, M. Ponec, J. Bouwstra, Acylceramide head group architecture affects lipid organization in synthetic ceramide mixtures, J. Invest. Dermatol. 123 (2004) 911–916.
[19] M.W. de Jager, G.S. Gooris, M. Ponec, J.A. Bouwstra, Lipid mixtures prepared with well-defined synthetic ceramides closely mimic the unique stratum corneum lipid phase behavior, J. Lipid Res. 46 (2005) 2649–2656.
[20] P.W. Wertz, D.T. Downing, Ceramides of pig epidermis: structure determination, J. Lipid Res. 24 (1983) 759–765.
[21] P.W. Wertz, D.T. Downing, Epidermal lipids, in: L.A. Goldsmith (Ed.), Physiology, Biochemistry and Molecular Biology of the Skin, Oxford University Press, Oxford, 1991, pp. 205–235.
[22] A. Weerheim, M. Ponec, Determination of stratum corneum lipid profile by tape stripping in combination with high-performance thin-layer chromatography, Arch. Dermatol. Res. 293 (2001) 191–199.
[23] J. Nijsse, A.C. van Aelst, Cryo-planing for cryo-scanning electron microscopy, Scanning 21 (1999) 372–378.
[24] W. Bras, A SAXS/WAXS beamline at the ESRF and future experiments, J. Macromol. Sci. Phys., B 37 (1998) 557–566.
[25] I.P. Dolbnya, H. Alberda, F.G. Hartjes, F. Udo, R.E. Bakker, M. Konijnenburg, E. Homan, I. Cerjak, P. Goedtkindt, W. Bras, A fast position sensitive MSGC detector at high count rate operation, Rev. Sci. Instrum. 73 (2002) 3754–3758.
[26] J.A. Bouwstra, G.S. Gooris, F.E.R. Dubbelaar, M. Ponec, Cholesterol sulfate and calcium affect stratum corneum lipid organization over a wide temperature range, J. Lipid Res. 40 (1999) 2303–2312.
[27] P.W. Wertz, D.T. Downing, Stratum corneum: biological and biochemical considerations, in: J. Hadgraft, R.H. Guy (Eds.), Transdermal Drug Delivery: Developmental Issues and Research Initiatives, Marcel Dekker, Inc., New York, 1989, pp. 1–22.
[28] J.P. Bradshaw, S.M.A. Davies, T. Hauss, Interaction of substance p with phospholipid bilayers: a neutron diffraction study, Biophys. J. 75 (1998) 889–895.
[29] J. Katsaras, S. Tristram-Nagle, Y. Liu, R.L. Headrick, E. Fontes, P.C. Mason, J.F. Nagle, Clarification of the ripple phase of lecithin bilayers using fully hydrated, aligned samples, Phys. Rev., E Stat. Phys. Plasmas Fluids Relat. Interdiscip. Topics 61 (2000) 5668–5677.
[30] M.W. de Jager, G.S. Gooris, I.P. Dolbnya, M. Ponec, J.A. Bouwstra, Modelling the stratum corneum lipid organisation with synthetic lipid mixtures: the importance of ceramide composition, Biochim. Biophysic. Acta 1664 (2004) 132–140.